



Semnan University



## Research Article

# Numerical Study of Membrane Humidifier Performance with Single Channel Serpentine Configuration on Both Wet and Dry Sides

Ebrahim Afshari <sup>a\*</sup>, Nabi Jahantigh <sup>b\*</sup>

<sup>a</sup> Department of Mechanical Engineering, Faculty of Engineering, University of Isfahan, Isfahan, Iran

<sup>b</sup> Department of Mechanical Engineering, Faculty of Engineering, University of Zabol, Zabol, Iran

## ARTICLE INFO

**Article history:**

Received: 2024-07-23

Revised: 2024-10-30

Accepted: 2024-11-29

**Keywords:**

Membrane humidifier;  
PEM fuel cell;  
Serpentine flow channels;  
Water transfer;  
Numerical modeling.

## ABSTRACT

The simplest and most prevalent method for water management inside proton exchange membrane fuel cells is the moisturization of hydrogen gas and air (or oxygen) before fuel cell entrance. To this end, membrane humidifiers with distinct specifications such as structural simplicity, no electric power consumption, and lack of moving parts are used. The current paper presents a study of such a humidifier and proposes building serpentine flow channels on the wet and dry sides to increase gas retention duration on the membrane surface. The humidifier's numerical 3D modeling was used to analyze several parameters, including water volume passage through the membrane, flow velocity inside channels, gas temperature on the dry and wet sides, and pressure drop inside channels. According to the results, water moves from the wet side to the dry side through the membrane, and water concentration increases along the channel on the dry side, such that the water concentration at the output on the dry side reaches 2.8 moles per cubic meter. Although serpentine flow channels cause more pressure drop compared to parallel channels, the longer gas retention duration inside the channels on both dry and wet sides improves the humidifier's performance in terms of heat transfer and water mass transfer.

© 2025 The Author(s). Journal of Heat and Mass Transfer Research published by Semnan University Press.

This is an open access article under the CC-BY-NC 4.0 license. (<https://creativecommons.org/licenses/by-nc/4.0/>)

## 1. Introduction

Among the various types of fuel cells, proton exchange membrane (PEM) fuel cells have attracted recent attention due to their advantages, including high power density, short startup duration, high efficiency, and low operation temperature. In this type of fuel cell, a polymer is used as the electrolyte, with its most important role being the transfer of protons produced from the anode to the cathode side. Since the membrane is used to transfer protons, it needs to be wet. Nevertheless, the amount of

water inside the fuel cell must be precisely controlled so that it does not exceed a particular ceiling or fall short of a certain floor. If there is too little water inside the cell, the membrane will dry out. Consequently, the proton conductivity of the membrane is reduced, and the membrane ion conduction will falter. As the cathode side's electrochemical reactions produce water, water shortage occurs most often on the anode side, though shortage remains an important effect on the cathode side as well, especially in the cell entrance region [1]. If the water in the cell

\* Corresponding author.

E-mail address: [e.afshari@eng.ui.ac.ir](mailto:e.afshari@eng.ui.ac.ir) & [njahantigh@uoz.ac.ir](mailto:njahantigh@uoz.ac.ir)

## Cite this article as:

Afshari, E. and Jahantigh, N., 2025. Numerical Study of Membrane Humidifier Performance with Single Channel Serpentine Configuration on Both Wet and Dry Sides. *Journal of Heat and Mass Transfer Research*, 12(2), pp. 247-258.

<https://doi.org/10.22075/JHMTR.2024.34827.1586>

exceeds a certain amount, the high humidity inside the cell causes the water to become saturated, and part of it will change to liquid. Liquid water can block some porosity, allowing a lower amount of gas to reach or transfer to the catalyst layer. Water management is thus essential for proper control of water inside a fuel cell. Among the various water management methods in the polymer membrane fuel cell, the simplest and most controllable method is gas humidification. A humidifier humidifies reactive gases before entering the fuel cell.

Among various humidifiers, membrane humidifiers are the most prevalent apparatuses for moisturizing, offering minimum energy consumption and a simple structure. Numerical modeling of humidifiers can help analyze the transfer phenomena governing a humidifier's nature and design. In membrane humidifiers, flow passage plates are installed on two sides of the membrane. The flow field created in these plates, which is used for the entrance of dry and wet gases into the humidifier, is important and can affect the moisturizing rate. The flow field usually consists of parallel or serpentine channels. Parallel channels are easier to build and feature a lower pressure drop. Due to a more uniform distribution of water and temperature on the membrane surface, serpentine channels increase humidifier efficiency. However, the pressure drop due to local drops in serpentine channels is greater than in parallel channels. Therefore, the analysis of serpentine channels can prove their usefulness and efficiency [2].

Several studies have analyzed the performance and control of membrane humidifiers. Chen and Peng [3] developed a dynamic model that included critical parameters such as pressure, flow rate, temperature, and relative humidity of air flow. Steady-state simulations were performed to optimize the humidifier design. Ahmadi-Taba et al. [4] built a bubble humidifier for moisturizing PEM fuel cell reactive gases. Chen and Peng [5] modeled and analyzed a membrane humidifier for moisturizing the anode side input. Their model consisted of four stages for careful observation of the moisturization behavior. Park and Oh [6] provided a 1D model for analyzing a membrane humidifier and the gas flow rate at the wet side of the humidifier. Kang et al. [7] used a 2D model of a membrane humidifier consisting of a shell and a pipe to analyze the moisturization performance. They concluded that the humidifier behavior is preferable for configurations with the same alignment but not for the same direction. Yu et al. [8] provided a steady model of heat and mass transfer, conducting a parameter study on a membrane humidifier's performance to attain an optimal design. Ramya et al. [9] compared the

performance of a bubble humidifier and a membrane humidifier used in a fuel cell. They found better performance for a membrane humidifier at higher current densities compared to a bubble humidifier, as it exerts less parasitic power. Afshari and Baharlou [10] developed a model for analyzing humidifier performance in two configurations: counter and parallel flows. In humidifiers with counterflow, water, and heat transfer are better than in the parallel flow configuration, leading to a higher dew point temperature in the dry region outlet. Ahluwalia et al. [11] used numerical modeling of a humidifier and found that water mass transfer from the wet side to the dry side was affected by the wet side's relative wetness at low pressures and mass transfer effects at high pressures. Cave and Merida [12] modeled a parallel-channel membrane humidifier to measure temperature and moisture profiles. It became clear that moisture transfer is affected by higher flow velocity from the inlet to the outlet. Pandey et al. [13] analyzed a mathematical model of the humidifier. They utilized a circular membrane with an empty inside, along with the humidifier. Chen et al. [14] performed lab research, analyzing heat and mass transfer in a membrane humidifier, and concluded that an increase in flow would increase water transfer throughout the membrane. Wang et al. [15] used a new method to optimize three-dimensional coolant channels for flow and heat transfer in a proton exchange membrane fuel cell by deep-learning accelerating topology. Yan et al. [16] studied the effect of channel dimensions and dry air inlet changes in conditions such as moisture on a humidifier, dew point temperature difference, and performance coefficient. Pang et al. [17] used a neural network of neutron radiography to analyze the water spatial distribution in polymer electrolyte membrane fuel cells.

To increase the gas retention duration on both sides of the humidifier membrane and thus enhance water transfer through the membrane, to uniformly distribute the wet and dry gases on the respective sides, and to improve temperature distribution on the membrane, the present study suggests the use of single serpentine flow channels instead of parallel channels in humidifiers. Using the pattern of single spiral channels leads to simultaneous uniformity of temperature and water distribution in the humidifier.

Gurau et al. [18], in one of their research, presented a two-dimensional model for proton exchange membrane fuel cells and investigated the temperature distribution and mass and heat transfer for said fuel cell. Through 3D numerical modeling, the performance of a serpentine channel humidifier, water passage through the

membrane, and the pressure drop inside the channels have been analyzed. Also, Wang et al. [20], in recent years, predicted the effective penetration of porous medium using deep learning method for use in fuel cell. Wang et al. [21] conducted a new study on the application of small-scale proton exchange membrane fuel cells. This study shows that small-scale fuel cells have been considered in industrial applications.

## 2. Plane Membrane Humidifier

Membrane humidifiers are the simplest and the most common type of humidifiers, used for moisturizing reactive gases in PEM fuel cells, as they feature minimal energy consumption and reduce fuel cell systemic complexity and its parasitic power. These humidifiers employ a polymer membrane which able them to pass moisture and heat without giving passage to gases. Figure 1 is a schematic of this type of humidifier.

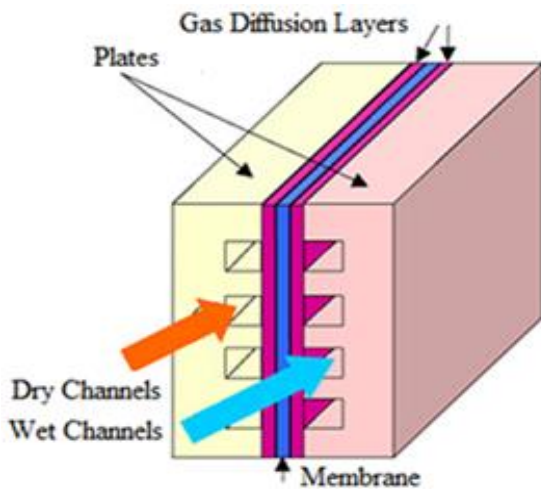


Fig. 1. Schematic display of membrane humidifier

As can be seen, there are channels inside the two metal or graphite plates designed to pass gases through. One of these plates' channels is dedicated to dry gases, while the channels in the other are for wet gases. A membrane located between the two plates plays the role of water transfer from the wet to the dry gas side. Water passage through the membrane and the transfer of water to the dry gas causes the gas to moisturize and allows it to be used in the fuel cell. Parallel channels are the most common flow paths within a humidifier. The pressure drop inside parallel channels is low. However, the gas retention duration inside these channels is low, and the opportunity to exchange water and heat between the dry and wet gas is limited. That's the reason why the use of serpentine flow channels is preferred. Serpentine channels distribute temperature inside humidifiers. The uniform

distribution of temperature over the humidifier will prevent the membrane from local dryups. When the wet gases enter one side of the membrane, water penetrates the entire membrane, ending up on the dry side. Membrane humidifiers are the simplest and most common type of humidifiers used for moisturizing reactive gases in PEM fuel cells, as they feature minimal energy consumption and reduce fuel cell systemic complexity and parasitic power. These humidifiers employ a polymer membrane that allows them to pass moisture and heat without giving passage to gases. Fig. 1 is a schematic of this type of humidifier. As can be seen, there are channels inside two metal or graphite plates designed to pass gases through. One of these plates' channels is dedicated to dry gases, while the channels in the other are for wet gases. A membrane located between the two plates facilitates water transfer from the wet to the dry gas side. Water passage through the membrane and the transfer of water to the dry gas causes the gas to moisturize, allowing it to be used in the fuel cell. Parallel channels are the most common flow paths within a humidifier. The pressure drop inside parallel channels is low. However, the gas retention duration inside these channels is also low, and the opportunity to exchange water and heat between the dry and wet gas is limited. These are the reasons why serpentine flow channels are preferred. Serpentine channels distribute temperature more evenly inside humidifiers. The uniform distribution of temperature over the humidifier prevents the membrane from local dry-ups. When wet gases enter one side of the membrane, water penetrates the entire membrane, ending up on the dry side.

## 3. Governing Equations

Figure 2 shows a schematic of a 3D humidifier model with serpentine flow channels. Serpentine channels are located on both dry and wet sides, with the membrane located between them.

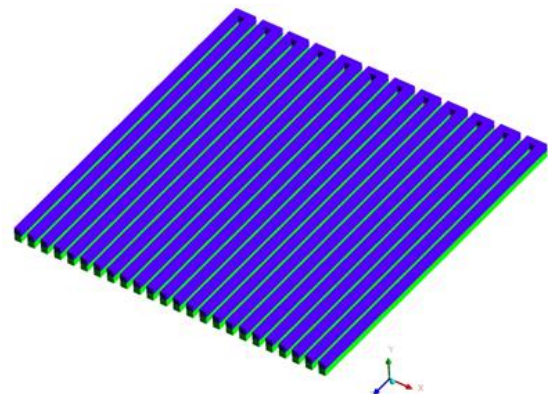


Fig. 2. Humidifier with serpentine flow channels

As the gas on the wet side enters the fuel cell working temperature, most of its moisture is in the gas phase. Since moisture transfer through the membrane is only possible via water vapor, the formation of small amounts of liquid water has little effect on moisture transfer. Other assumptions include the gases are ideal gases; the flow is steady-state, laminar, and incompressible. The membrane structure is uniform and homogeneous. The humidifier is completely insulated, forcing heat transfer to occur only through the membrane. According to these assumptions, the governing equations for the membrane humidifier include conservation of mass flow (Eq. 1), momentum (Eq. 2), species (Eq. 3), and energy (Eq. 4). These equations are presented as follows.

$$\nabla \cdot (\rho \vec{u}) = 0 \tag{1}$$

$$\frac{1}{\varepsilon^2} \nabla \cdot (\rho \vec{u} \vec{u}) = -\nabla p + \nabla \cdot \tau + S_{Dar} \tag{2}$$

$$\nabla \cdot (\vec{u} C^i) = \nabla \cdot (D^{i,eff} \nabla C^i) \tag{3}$$

$$\nabla \cdot (\rho c_p \vec{u} T) = \nabla \cdot (k^{eff} \nabla T) \tag{4}$$

where,  $\vec{u}$  is the velocity vector and  $\rho$  is the gas mixture density. These equations hold true for both the membrane and the channels. In the momentum conservation equation,  $p$  and  $\mu$  represent pressure and viscosity, respectively.  $\varepsilon$  is the porous medium's porosity coefficient. The porosity is 0.5 in the membrane and 1 in the channels. In the species conservation equation,  $C_i$  is the molar concentration of species  $i$ ,  $D_i^{eff}$  is the effective mass diffusivity of species  $i$  in the gas mixture.

The diffusion coefficient in the channels is obtained from the following equation [22]

$$D^{i,eff} = D_0 \left(\frac{T}{T_0}\right)^{1.5} \left(\frac{P_0}{P}\right) \tag{5}$$

in the above equation,  $D^i$  is the diffusion coefficient of particle "i" in the gas mixture and  $D_0$  the diffusion coefficient is at  $T_0$   $T_0$  and  $P_0$ .

The flow rate of water passing through the membrane is obtained from the following equation.

$$\dot{m}_m = \frac{\rho_{m,dry}}{W_{m,dry}} A_m M_{H_2O} D_m^{H_2O} \nabla \lambda \tag{6}$$

where,  $\dot{m}_m$  is the flow rate of water passing through the membrane,  $\rho_{m,dry}$  is the dry density of the membrane,  $W_{m,dry}$  is the dry equivalent weight of the membrane,  $A_m$  is the area of the membrane and  $M_{H_2O}$  is the molar mass of water.

The water diffusion coefficient in the membrane is expressed by the following equation [23].

$$D_m^{H_2O} = \begin{cases} 3.1 \times 10^{-7} \lambda (e^{0.28\lambda} - 1) \cdot e^{(-2346/T)} \lambda \leq 3 \\ 4.17 \times 10^{-8} \lambda (1 + 161e^{-\lambda}) \cdot e^{(-2346/T)} other \end{cases} \tag{7}$$

where,  $\lambda$  is the water capacity of the membrane.

$$\lambda = \begin{cases} 0.043 + 17.81a - 39.85a^2 + 36.0a^3 \\ 14 + 1.4(a - 1) for 1 < a \leq 3 \end{cases} \tag{8}$$

In the above relation,  $a$  is the activity of water vapor and it is defined as follows:

$$a = \frac{C^{H_2O} RT}{P_{sat}} \tag{9}$$

in the above equation,  $C^{H_2O}$  is water concentration in the membrane. It is defined as follows [23].

$$C^{H_2O} = \frac{\lambda \rho_{m,dry}}{W_{m,dry}} \tag{10}$$

where  $T$  is the temperature in degrees Celsius,  $\rho_{m,dry}$  is the dry density of the membrane and  $W_{m,dry}$  is the dry equivalent weight of the membrane. In the simulation, the dry density of the membrane is 2000 kg/m<sup>3</sup> and the dry equivalent weight of the membrane is 1.1 kg/mol. Also, in equation (8),  $P_{sat}$  is the saturation pressure. It is obtained from the following equation.

$$P_{sat} = 0.61078 \exp\left(\frac{17.27T}{T + 237.3}\right) \tag{11}$$

where,  $T$  is the temperature in degrees Celsius and  $P$  is in kPa.

In the energy equation,  $c_p$  is the specific heat capacity and  $k^{eff}$  is the effective thermal conductivity.

$$k^{eff} = \frac{1}{\frac{1-\varepsilon}{3k_m} + \frac{\varepsilon}{2k_m} + k_w} - 2k_m \tag{12}$$

## 4. Boundary Conditions and Numerical Solution Methods

### 4.1. Boundary Conditions

Either a single-domain or multi-domain method can be used in the numerical modeling of the humidifier. A study by Gurau et al. [18] was performed based on a multi-domain method in which the calculation domain is divided into several subdomains. A set of conservation

equations, including mass flow, momentum, species, and energy conservation equations, is then solved for each subdomain. To solve these equations and find their relationships with one another, boundary conditions between different domains of the humidifier are needed. However, many of these boundary conditions are not clear, and the answers obtained from solving the equations are often inaccurate. In the single-domain method, only some conservation equations are used across all domains. In this method, there is no need to specify boundary conditions at the intersections of domains.

In this model, a single region method is used. Therefore, only the external boundary conditions should be determined, and there is no need for boundary conditions between the membrane and the humidification channels. In the inlets on the wet and dry sides, the flow rate of the inlet flow for the dry and wet sides is equal to that of the dry side. It is equal to 9 mg/s. The temperature of the inlet dry and wet side gases is 303 and 353 K, respectively. The flow at the outlet boundaries is considered developed or zero flux with back pressure. On the walls, the no-slip condition is used for the velocity, and the zero flux condition is used for other variables. The inlet temperature in both dry and wet channels is considered a constant value, and the external walls of the humidifying unit are defined as isolated (zero flux). Other geometric and functional conditions are presented in Table 1.

**Table 1.** Geometrical, functional, transfer parameters and properties of membrane moisturizing materials

Geometrical Parameters	Symbol	Unit	Value
Length of channel (humidifier length)	L	mm	5
Cross section of channel	W	mm	2
Height of channel	H	mm	2
Rib of channel	D	mm	2
Total height of humidifier	H	mm	5
Total width of the humidifier	W	mm	5
Membrane thickness	th	micro meter	25
Dry side inlet temperature	T	K	303
Wet side inlet temperature	T	K	353
Wet side/dry side pressure	P	KPa	151.97

Relative humidity of the dry side inlet	$\phi$	-	0
Relative humidity of wet side inlet	$\phi$	-	1
Inlet flow to dry and wet channels	M	mg/S	9
Viscosity	$\mu$	Pa. S	$1.88 \times 10^{-5}$
Thermal conductivity coefficient of air	K	W/mK	0.0028
Thermal conductivity coefficient of water	K	W/mK	0.024
Thermal conductivity coefficient of the membrane (nafion)	K	W/mK	0.95
Oxygen diffusion coefficient at 1.5 atm and 353 K	D	m <sup>2</sup> /s	$1.806 \times 10^{-5}$
Water diffusion coefficient at 1.5 atm and 353 K	D	m <sup>2</sup> /s	$2.236 \times 10^{-5}$
Dry density of the membrane	$\rho_{m,dry}$	kg/m <sup>3</sup>	1980
Dry equivalent weight of the membrane	$W_{m,dry}$	kg/mol	1
Membrane permeability	K	m <sup>2</sup>	$10^{-12}$
Membrane porosity coefficient	$\epsilon$	-	0.5

#### 4.2. Numerical Solution Methods

Governing equations of the humidifier have been discretized through the finite volume method and solved using Ansys software. Velocity and pressure fields have been obtained through the SIMPLE algorithm. A double-sided gradient stability method, a W-cycle for the conservation equations, and an F-cycle for other equations have been utilized. Solution convergence scales are set based on the diagram for mass ( $10^{-4}$ ) and energy ( $10^{-6}$ ) equation residuals. Network independence has been studied by changing the number of nodes in all regions.

The problem was solved for several different grid sizes for its independency. In the Fig. 3 the changes of water molar concentration along the dry air channel are plotted for the various number of grid cells. As shown the final results are independent numbers of grids because there is no change in the results by increasing the number of grid cells to 2,200,000.

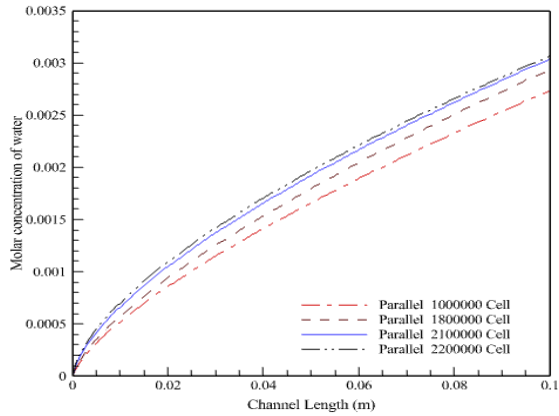


Fig. 3. The effects of the cell number on water molar concentration along the dry air channel

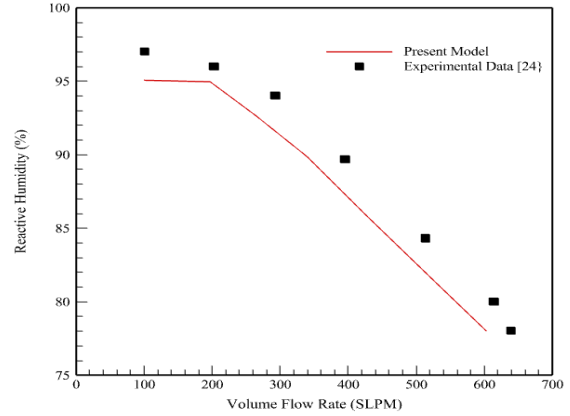


Fig. 5. Comparison of present numerical model results of membrane humidifier and Experimental data [24]

### 5. Results

To verify the numerical modeling of the humidifier, a model with parallel flow channels is used. Here, a model with parallel flow channels is simulated, and the numerical results are compared with similar experimental results from reference [19]. To ensure the accuracy of the numerical simulation, the output relative humidity variation diagram on the dry side against input mass flow rate is compared to experimental results for a similar humidifier, as both humidifiers operate under the same input conditions. As can be seen from Fig. 4, there is good agreement between the derived and experimental results.

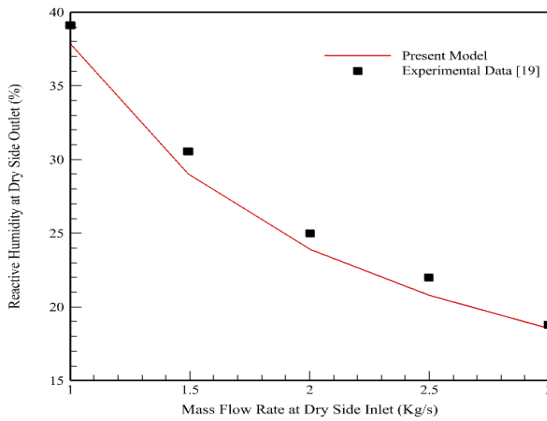


Fig. 4. Comparison of the relative humidity of dry side outlet with the experimental datas [19]

The difference between the results can be attributed to the assumption of a single-phase numerical model. It must be noted that although the amount of liquid water is low, this small amount of water has affected the performance and caused a difference between the results of numerical simulation and experimental data.

In order to further ensure the results of numerical modeling, the present model with different dimensions and performance conditions 4 has been validated with experimental data [24] in Fig. 5.

The flow field in experimental data is simple parallel. All functional and physical dimensions and conditions in both models are similar together. There is about 6% error between the experimental and numerical results. Comparing the results shows that the results of the current numerical model are accurate enough.

In Fig. 6, the molar concentration variation of water along the dry and wet sides is displayed. According to Fig. 6a, water is transferred through the membrane from the wet side to the dry side, and the molar concentration of water along the channel increases on the dry side in such a way that water concentration at the dry side outlet reaches 2.8 moles per cubic meter.

More diffusion of water through the membrane causes the water concentration to increase along the channels on the dry side. Along wet channels; The concentration of water is reduced; As a result, the water transfer from the wet side to the dry side decreases along the length of the channel. Therefore, the changes in water concentration at the beginning of the canals on the dry side are greater than at the end of the canals.

Water concentration at the dry side inlet is zero, meaning that the gas entering the dry side has been dehydrated. As shown in Fig. 6b, as water on the wet side has migrated through the membrane, water concentration along the channel on the wet side has reduced from 13.6 to 11.7. The forward and backward paths for wet and dry air have caused gas retention time in wet and dry channels to increase, providing sufficient time and opportunity for the proper transfer of water from the wet side to the membrane and from the membrane to the dry side. In the bend regions of the channels, which are numerous, gas flow velocities on both dry and wet sides reduce. This leads to more opportunities for water transfer between the dry and wet sides, resulting in more water being transferred to the dry side.

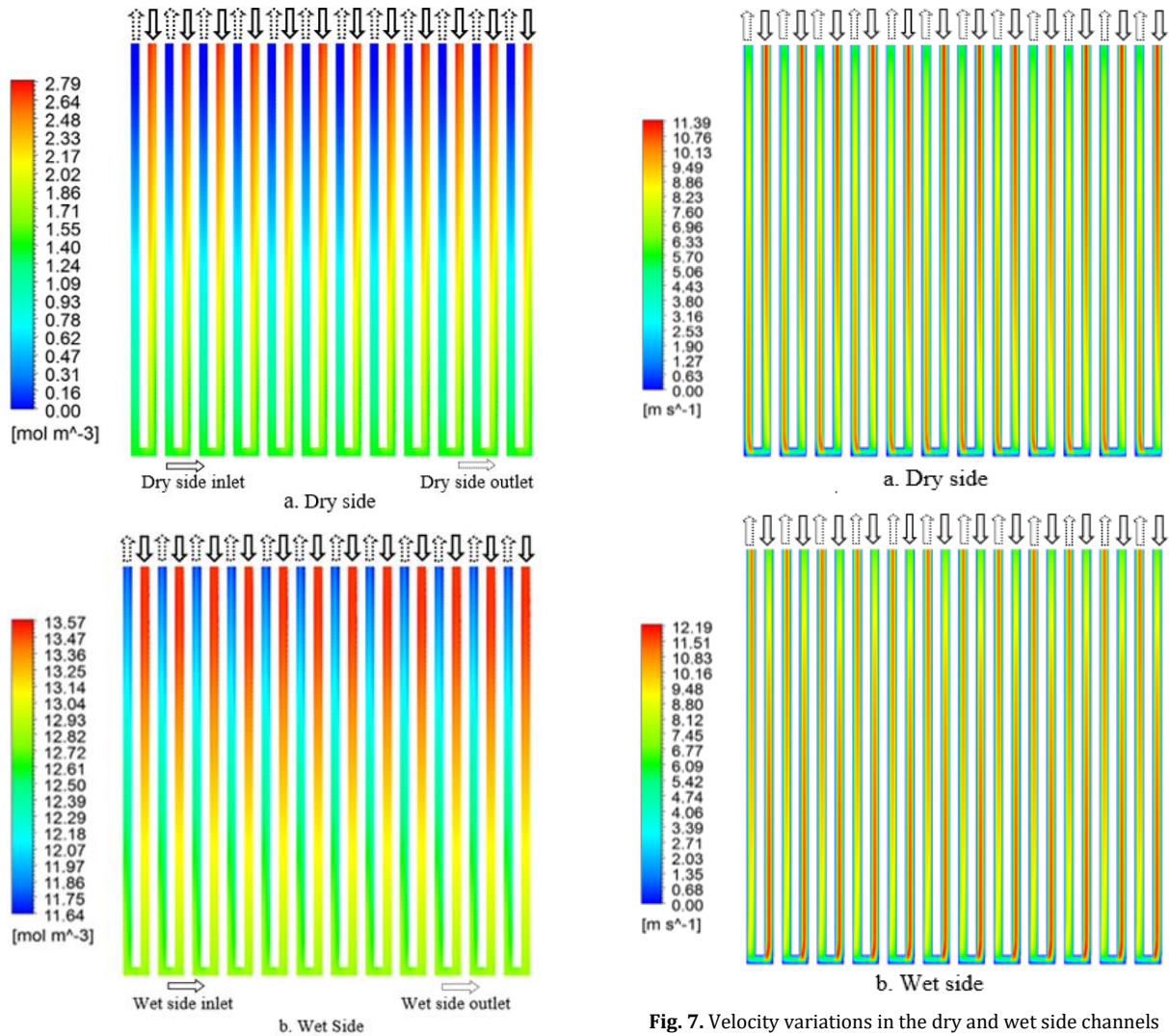


Fig. 6. Water molar concentration variation on the dry and wet sides

Fig. 7. Velocity variations in the dry and wet side channels

Figure 7 displays the velocity distribution in the middle section of the dry and wet channels. The average velocities at the dry side inlet and the wet side inlet are 5.1 and 6.6 m/s, respectively. A higher mass flow rate is the reason why the wet channel velocity is higher. As the channel length is longer on both dry and wet sides, the flow at these channels' outlets is fully developed. According to Fig. 7a, water entrance from the wet side to the dry side causes flow velocities inside the dry side channels to increase accordingly. The water entrance into the dry side channels reduces air mixture density and water vapor content, potentially causing a decrease in fluid velocity on the dry side. However, the velocity drop caused by density reduction is negligible compared to the velocity increment caused by flow rate increase on the dry side, which is why fluid velocity increases along the dry side channels.

The density changes of the gas mixture on the dry side (air and water vapor) depend on the flow rate of the gases on the dry side. In low flow rates of gases, these effects are more, and they are less in high flow rates.

The velocity of the air and water vapor mixture decreases in the bend regions of channels, meaning that in-channel gas retention duration has increased and exchange opportunities between dry and wet regions have improved. According to Fig. 7, the velocity variation trend along the wet side channels is opposite to that of the dry side channels, meaning the air and water vapor mixture's velocity decreases as it moves along the channels. It occurs for two reasons;

- 1) water transfer from the wet side to the dry side decreases the mass flow on the wet side, leading to a decrease in velocity on the wet side.
- 2) water transfer from the wet side to the dry side increases the air and water vapor mixture density along the channels, which in turn decreases the air and water vapor mixture fluid velocity.

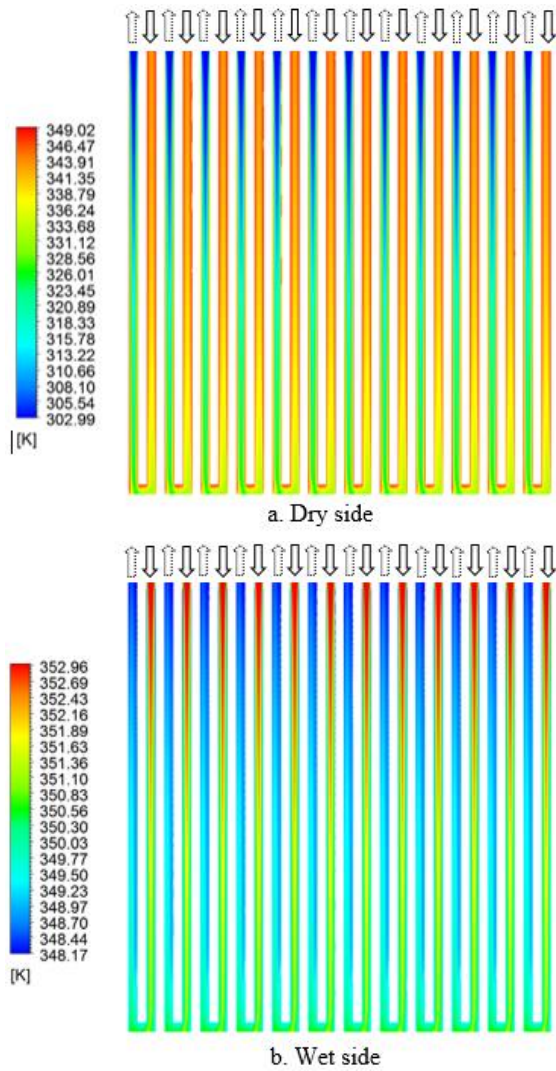


Fig. 8. Temperature variation in dry and wet side channels for serpentine flow arrangement

Figure 8 displays the temperature variation along the serpentine flow channel on both dry and wet sides. According to Fig. 8a, dry gas enters the channels at a temperature of 300K and leaves at a temperature of 349K. The rise in dry gas temperature occurs for two reasons: First, the fluid on the wet side is warmer than the dry side's fluid. Heat transfers from the wet side to the dry side. The temperature of fluid on the wet side increases. The second reason is the transfer of water from the wet side to the dry side, leading to an increase in the net enthalpy and the amount of fluid on the dry side. Achieving a uniform distribution of temperature on the dry and wet sides is not feasible. However, temperature distribution on the dry side is relatively uniform. Uniform distribution of temperature on the dry and wet sides will increase the membrane lifetime. According to Fig. 8b, the temperature variation trend on the wet side is the opposite of the dry side, and the two factors mentioned above cause a rechanneling in the fluid temperature on the wet side. However,

temperature variation on the wet side is much lower than temperature change on the dry side. This is because the gas flow and water heat capacity are higher on the wet side than on the dry side. It must be noted that not only can the membrane transfer water, but it can also transfer heat. As the relative humidity of gas on the dry-side input depends on the amount of water in the gas, it also depends on the dry side outlet. Thus, through temperature control, dry side relative humidity can also be controlled. If the water transfer through the membrane is not too high, temperature control in the membrane humidifier allows outlet gas moisture control on the dry side. The primary head drops due to local resistance will cause a pressure drop along the channels. We are thus interested in the pressure drop in channels expected to be the lowest. As explained in Fig. 4, the bends region will cause an increase in pressure drop in the humidifier.

In Figs. 9a and 9b, variations in pressure along the dry and wet side channels are displayed.

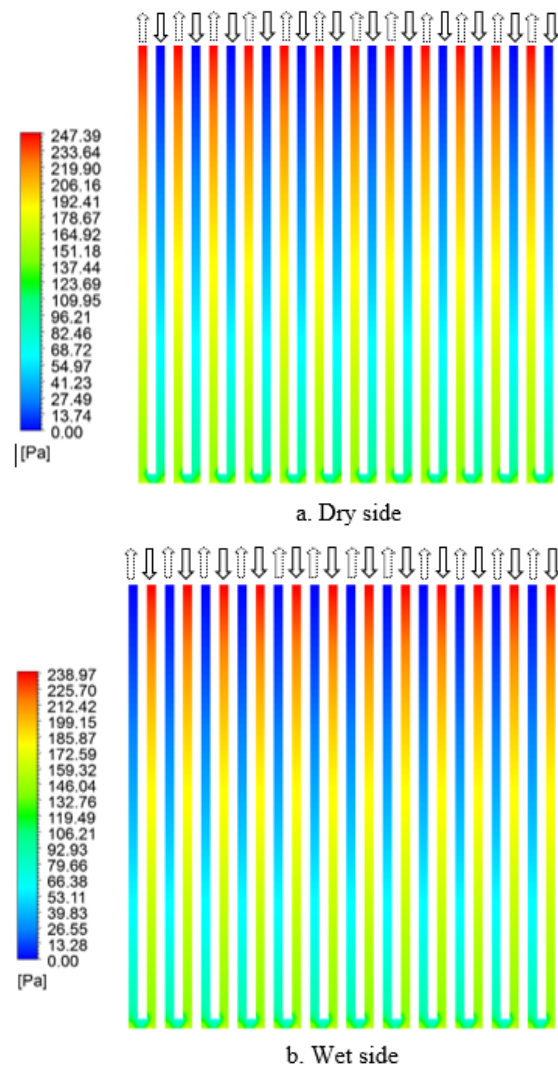


Fig. 9. Pressure variation in dry and wet side channels for serpentine flow arrangement



It is evident that the channel length in the serpentine flow configuration is greater than that in the parallel configuration. Pressure drop due to friction with the channel walls is much higher in the serpentine flow channels than in the parallel configuration. In fact, when designing serpentine and parallel channels, one must balance the pressure drop against the amount of water transferred through the membrane from the wet side to the dry side. However, water transfer is not just a critical parameter in a humidifier but is, in fact, its key objective. Thus, serpentine flow channels on both sides improve performance, even though they lead to a higher pressure drop in the channels. Comparing Fig. 9a and Fig. 9b, it is apparent that the pressure drop on the dry side is higher than on the wet side. This is due to the water transfer from the wet side to the dry side, which results in an increase in the flow rate on the dry side.

One of the important parameters in the humidifier performance is the inlet flow field characteristics. In order to investigate the effect of inlet flow conditions on its performance, the effect of temperature and flow rate of inlet dry air, which are two basic parameters in the design of the humidifier, has been conducted on the performance of the humidifier that other parameters are constant. The flow rate and inlet temperature of the dry side are the parameters that the user chooses the humidifier with them. In order to investigate the effect of mass flow rate and inlet temperature of the dry side on the performance of the humidifier, the temperature is considered between 20 and 40 degrees Celsius, and the mass flow rate is between 0.34 and 0.51 mg/s.

In Fig. 10, changes in the molar concentration of water at the outlet of the dry side are plotted along the inlet temperature at the dry side at the various flow rates.

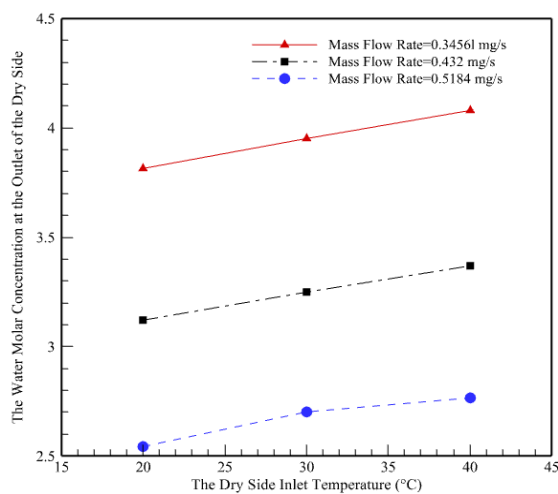


**Fig. 10.** The water molar concentration at the outlet of the dry side channels along the dry side inlet temperature at various mass flow rate

As can be seen, with the increased flow of dry air, the amount of moisture added to it has decreased. By increasing the flow rate and consequently increasing the flow velocity on the dry side, the residence time of the gas will decrease, and the gas will have less opportunity to absorb moisture. Then, the molar concentration of water in the outlet drops. Also, at a constant dry inlet air flow rate, with the increase in air temperature, the amount of water concentration in the outlet of the dry side has increased. This indicates the transfer of more water from the dry side to the wet side, and as a result, the temperature of the outlet of the dry side increases.

Temperature is an important parameter in the performance of the humidifier and can directly affect the transfer of water and heat. In Fig. 11, the temperature changes at the outlet of the dry side are plotted along the inlet temperature of the dry side at the various of the flow rate.

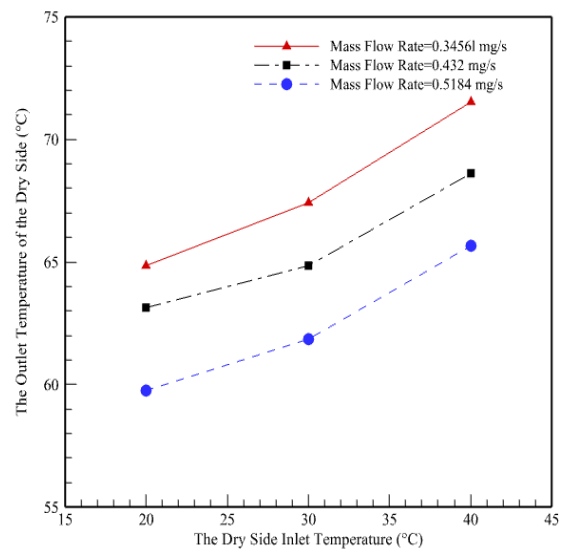


**Fig. 11.** Outlet temperature of the dry side channels along the dry side inlet temperature at various mass flow rate

According to Fig. 11, with the increasing the inlet temperature of the dry side, the temperature in the dry side outlet has increased. Also, with the increase in the mass flow rate of the dry side, the temperature at its outlet has decreased due to the reduction of the residence time of the flow in the dry side.

Figure 12 shows the changes in relative humidity at the outlet of the dry side channels along the inlet temperature of the dry side channels at various mass flow rates.

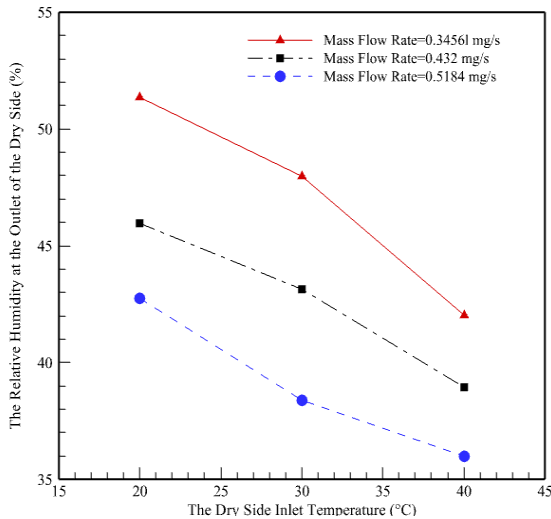


Fig. 12. The relative humidity at the outlet of the dry side channels along the dry side inlet temperature at various mass flow rate

According to the Fig. 12 as the dry side inlet temperature increases, the relative humidity at the dry side outlet decreases. The capacity of air increases as its temperature increases. When the temperature of the air increases it is possible to absorb the more moisture. The more water must be transferred to be the relative humidity constant.

Figure 13 shows the average pressure drop in the dry side channels along the inlet temperature of the dry side channels various the mass flow rate. As can be seen, with the increase in mass flow rate and consequently the increase of the flow velocity, the pressure drop increases. As the inlet temperature of the dry side increases, the pressure drop increases very little. The effect of mass flow rate increase on pressure drop is much higher than the effect of temperature increase on it.

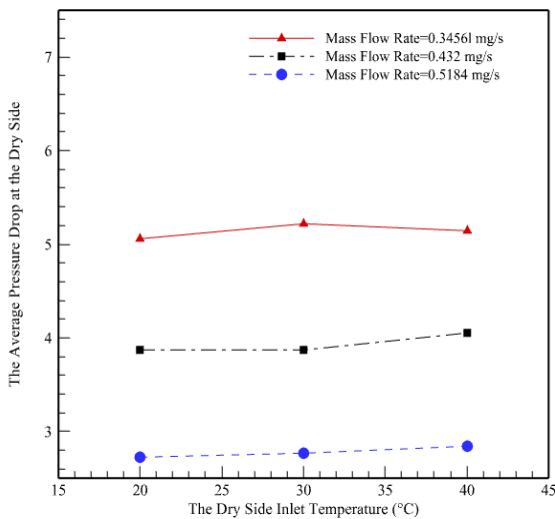


Fig. 13. Average pressure drop at dry side channels along the dry side inlet temperature at various mass flow rate

## 6. Conclusions

To improve gas retention duration on both sides of the membrane and consequently enhance the transfer of water and heat through the membrane, the present study proposes the employment of serpentine channels on both sides of membrane humidifiers. To this end, a membrane humidifier with serpentine flow channels on both dry and wet sides has been numerically modeled in three dimensions. Analysis findings are as follows:

1. The presence of bends in serpentine channels leads to increased gas retention duration on both dry and wet sides. Water transfer from the wet to the dry side naturally increases, enhancing membrane performance.
2. Considering that the membrane transfers not only water but also heat from the wet side to the dry side, it has been demonstrated that the presence of bent corners in the serpentine flow channels improves both the water transfer rate and the heat transfer rate from the warm side to the cool side. As the relative humidity on the humidifier's dry side depends on temperature and the amount of water, controlling heat transfer from the warm side to the cool side will lead to control over the gases relative humidity.
3. Although the bends in serpentine channels improve performance relative to parallel channels, these bends exacerbate pressure drop inside the channels, making it necessary to use a higher compressor power output to provide the humidifier with sufficient dry and wet gases. Results demonstrate that the additional pressure drop is, in fact, not significant. The use of serpentine flow channels on both dry and wet sides of membrane humidifiers is therefore recommended.
4. As the dry side inlet temperature increases, the moisture and relative humidity at the dry side outlet decreased and the temperature in the dry side outlet has increased. The effect of mass flow rate increase on pressure drop is much higher than effect of temperature increase on it.

## Nomenclature

$A_m$	Membrane area (m <sup>2</sup> )
$a$	Water vapor activity
$C$	Concentration (kmol/m <sup>3</sup> )
$cp$	Specific heat capacity (J/kg.K)
$D$	Diffusion coefficient (m <sup>2</sup> /s)
$e$	Exponential function
$K$	Permeability of porous medium (m <sup>2</sup> )
$k$	Thermal conductivity coefficient (W/m.K)
$M_{H_2O}$	Molar mass of water (g/mol)
$\dot{m}_m$	Flow rate of water passing through membrane (kg/s)
$P$	Pressure (Pa)
$S$	Source term
$T$	Temperature (K)
$u$	Velocity (m/s)
$W_{m,dry}$	Dry equivalent weight of the membrane
$\rho$	Density (kg/m <sup>3</sup> )
$\varepsilon$	Porosity coefficient
$\mu$	Dynamic viscosity coefficient (Pa.s)
$\lambda$	Membrane water coefficient
$\tau$	Shear Stress (Pa)
$\rho_{m,dry}$	Dry density of the membrane (kg/m <sup>3</sup> )
$\varphi$	Relative humidity
$\nabla$	Operator

## Funding Statement

This research did not receive any specific grant from funding agencies in the public, commercial, or not-for-profit sectors.

## Conflicts of Interest

The author declares that there is no conflict of interest regarding the publication of this article.

## Authors Contribution Statement

Ebrahim Afshari: Formal Analysis Investigation; Methodology; Project Administration; Software; Validation; Writing – Review & Editing.

Nabi Jahantigh: Formal Analysis; Software; Writing – Original Draft; Writing – Review & Editing.

## References

- [1] Huizing, R., 2007. Design and membrane selection for gas to gas humidifiers for fuel cell applications, University of Waterloo.
- [2] Najmi, A. H., et al., 2021. Experimental investigation and optimization of proton exchange membrane fuel cell using different flow fields. *Energy*, 217, p. 119313.
- [3] Chen, D., and Peng, H., 2005. A thermodynamic model of membrane humidifiers for PEM fuel cell humidification control. *Journal of Dynamic Systems, Measurement, Control*, 127, pp.424-432.
- [4] Ahmaditaba, A. H., Afshari, E., and Asghari, S., 2018. An experimental study on the bubble humidification method of polymer electrolyte membrane fuel cells. *Energy Sources, Part A: Recovery, Utilization, and Environmental Effects*, 40(12), pp. 1508-1519.
- [5] Chen, D., and Peng, H., 2008. Nonminimum-Phase Phenomenon of PEM Fuel Cell Membrane Humidifiers. *Journal of Dynamic Systems, Measurement, and Control*, 130, pp. 044501-044510.
- [6] Park, S., and Oh, I., 2009. An analytical model of Nafion TM membrane humidifier for proton exchange membrane fuel cells. *Journal of Power Sources*, 188, pp. 498-501.
- [7] Kang, S., Min, K., and Yu, S., 2010. Two dimensional dynamic modeling of a shell-and-tube water-to-gas membrane humidifier for proton exchange membrane fuel cell. *International Journal of Hydrogen Energy*, 35, pp. 1727-1741.
- [8] Yu, S., Im, S., Kim, S., Hwang, J., Lee, Y., Kang, S., et al., 2011. A parametric study of the performance of a planar membrane humidifier with a heat and mass exchanger model for design optimization. *International Journal of Heat and Mass Transfer*, 54, pp. 1344-1351.
- [9] Ramya, K., Sreenivas, J., Dhathathreyan, K.S., 2011. Study of a porous membrane humidification method in polymer

- electrolyte fuel cells. *International Journal of Hydrogen Energy*, 36, pp. 14866–72.
- [10] Afshari, E. and Baharlou Houreh, N., 2014. Performance analysis of a membrane humidifier containing porous metal foam as flow distributor in a PEM fuel cell system. *Energy Conversion and Management*, 88, pp. 612–621.
- [11] Ahluwalia, R.K., Wang, X., Johnson, W.B, Ber, F.G. and Kadylak, D., 2015. Performance of a cross-flow humidifier with a high flux water vapor transport membrane. *Journal of Power Sources*, 291, pp. 225–238.
- [12] Cave, P., and Mérida W., 2008. Water flux in membrane fuel cell humidifiers: Flow rate and channel location effects. *Journal of Power Sources*, 175, pp. 408–418.
- [13] Pandey, R., and . Lele, A, 2018. Modelling of water-to-gas hollow fiber membrane humidifier, *Chemical Engineering Science*, 192, pp. 955-971.
- [14] Chen, C.Y., Yan, W.M., Lai, C.N., and Su, J.H., 2017. Heat and mass transfer of a planar membrane humidifier for proton exchange membrane fuel cell. *International Journal of Heat and Mass Transfer*, 109, pp. 601-608.
- [15] Wang, Y., et al., 2023. Deep-learning accelerating topology optimization of three-dimensional coolant channels for flow and heat transfer in a proton exchange membrane fuel cell. *Applied Energy*, 352, p. 121889
- [16] Yan, W.M., Chen, C.Y, Jhang, Y.K., Chang, Y.H., Amani, P., and Amani M., 2018. Performance evaluation of a multi-stage plate-type membrane humidifier for proton exchange membrane fuel cell. *Energy conversion and management*, 176, pp. 123-130.
- [17] Pang, Y., Wang, Y., 2023. Water spatial distribution in polymer electrolyte membrane fuel cell: Convolutional neural network analysis of neutron radiography. *Energy and AI*, 14, p. 100265
- [18] Gurau, V., Liu, H., and Kakac, S., 1998. Two-dimensional model for proton exchange membrane fuel cells. *J. AIChE*, 44, pp. 2410-2422.
- [19] Houreh, N.B., Ghaedamini, M., Shokouhmand, H., Afshari, E., and Ahmaditaba, A.H., 2020. Experimental study on performance of membrane humidifiers with different configurations and operating conditions for PEM fuel cells. *International Journal of Hydrogen Energy*, 45(8), pp. 4841-4859
- [20] Wang, Z., et al., 2020. Prediction of effective diffusivity of porous media using deep learning method based on sample structure information self-amplification. *Energy and AI*, 2, p. 100035.
- [21] Wang, Z., et al., 2023. Application progress of small-scale proton exchange membrane fuel cell, *Energy Reviews*, 2, p. 100017.
- [22] Masaeli, N., Afshari, E., Baniasadi, E., and Baharlou-Houreh, N., 2023. Performance studies of a membrane-based water and heat exchanger using serpentine flow channels for polymer electrolyte membrane fuel cell application. *Applied Thermal Engineering*, 222, p. 119950.
- [23] Shamsizadeh, P., and Afshari E., 2022. Numerical modeling of a membrane humidifier for mechanical ventilation. *International Communications in Heat and Mass Transfer*, 132, pp. 105931.
- [24] Hwang, J.J., Chang, W.R, Kao, J.K., Wu, W., 2012. Experimental study on performance of a planar membrane humidifier for a proton exchange membrane fuel cell stack. *Journal of Power Sources*, 215, pp. 69–76.